Biodesign

pISSN 2288-6982 | eISSN 2288-7105

MINI REVIEW P 28-31

Crystallization and preliminary diffraction analysis of dual specificity phosphatase 13a

Hee Gyeong Min, Tae Jin Jeon, Chun Hwa Wei, Myungbin Kim and Seong Eon Ryu*
Department of Bioengineering, College of Engineering, Hanyang University, Seoul, Korea
*Correspondence: ryuse@hanyang.ac.kr

Dual specificity phosphatases (DUSPs) include MAP kinase phosphatases and atypical dual specificity phosphatases, and mediate cell growth and differentiation. They are considered as drug targets against cancers, diabetes, immune diseases, and neuronal diseases. Two different DUSPs, DUSP13a and DUSP13b are coded in one gene (*DUSP13*) whose alternative splicing results in two sequence-related proteins with different target specificities. The crystal structure of DUSP13b showed a canonical DUSP fold. However, the structure of DUSP13a has not been determined yet. To understand structural mechanism of distinctive target specificities of sequence-related DUSPs, we prepared diffraction-quality crystals of DUSP13a. Cysteine residues in DUSP13a gene were mutated to serine or alanine to prevent cysteine oxidation. From the stabilized protein, we were able to grow good crystals that diffracted to 1.7 Å resolution. The preliminary diffraction analysis revealed that the crystal is in the space group $P2_1$ with unit cell parameters of a = 40.04 Å, b = 89.34 Å, c = 45.90 Å, α = 90.00°, β = 89.87° and γ = 90.00°.

INTRODUCTION

Dual specificity phosphatases (DUSPs) are members of the protein tyrosine phosphatases (PTPs) family. PTPs dephosphorylate phosphor-tyrosine and phosphor-serine/threonine of target proteins and regulate cellular signal transduction involved in cell growth, differentiation and cell death (Alonso and Pulido, 2016; Tonks, 2006). DUSPs are classified into six subgroups based on sequence similarity: PRLs (phosphatases of regenerating liver), Cdc14 phosphatases (Cdc represents a cell division cycle), PTENs (phosphatase and tensin homologs deleted on chromosome 10), myotubularins, MKPs (mitogen-activated protein kinase phosphatases) and atypical DUSPs (Patterson et al., 2009).

Due to their functions in critical cellular processes, DUSPs are considered as targets for therapeutic drug developments against cancers, diabetes, immune diseases, and neuronal diseases (Bermudez et al., 2010; Keyse, 2008; Patterson et al., 2009). In particular, DUSPs play a main role in cell growth and survival by regulating map kinase (MAPK) signaling pathway by dephosphorylating MAPK proteins such as ERK, JNK and p38. DUSPs are subdivided into typical and atypical groups. Typical DUSPs contain MAPK binding domain (MKB) as a regulatory domain, while atypical DUSPs lack the regulatory MKB domain. Atypical DUSPs, like typical DUSPs, can dephosphorylate MAPK and play a role in cell growth, apoptosis and cell signaling.

The active site of PTPs consists of the conserved P-loop and WPD-loop (the D-loop in DUSPs). These loops perform a key role in the activity mechanism of PTPs (Pavic et al., 2015; Wiesmann et al., 2004). The active site pocket of DUSPs is shallower than that of classical PTPs to fit the short side chains of phosphor-serine/threonine as well as the long side chains of phosphor-tyrosine (Jeong et al., 2014; Yuvaniyama et al., 1996). DUSP13a is an atypical DUSP and lacks the N-terminal regulatory domain found in MKPs (Patterson et al., 2009). Two different DUSP13s, DUSP13a (MDSP, muscle-restricted DUSP) and DUSP13b (TMDP, testis and skeletal muscle specific DUSP) are coded in one gene (*DUSP13*) whose alternative splicing results in two different proteins with highly similar amino acid sequences (Chen et al., 2004).

DUSP13a induces activity of apoptosis signal-regulating kinase 1 (ASK1) and knockout of DUSP13a inhibits activation of ASK1 and cellular apoptosis (Park et al., 2010). In comparison, DUSP13b regulates activation of JUN and p38 kinases (Katagiri et al., 2011; Nakamura et al., 1999). The crystal structure of DUSP13b showed the canonical DUSP fold without indicating particular information on the substrate specificity (Kim et al., 2007). To understand determinants of target specificity of two DUSPs with high sequence homology, atomic-level structures of both DUSP13a and 13b are required. For the structural studies of DUSP13a, we performed purification and crystallization of DUSP13a. To obtain stable proteins that could yield successful crystallization, cysteine residues in DUSP13a gene were mutated to serine or alanine. From the stabilized DUSP13a, we were able to obtain good crystals that diffracted to 1.7 Å resolution.

RESULTS AND DISCUSSION

The cDNA coding for human DUSP13a (residues 1-185) was cloned and expressed by using an *E.coli* over-expression

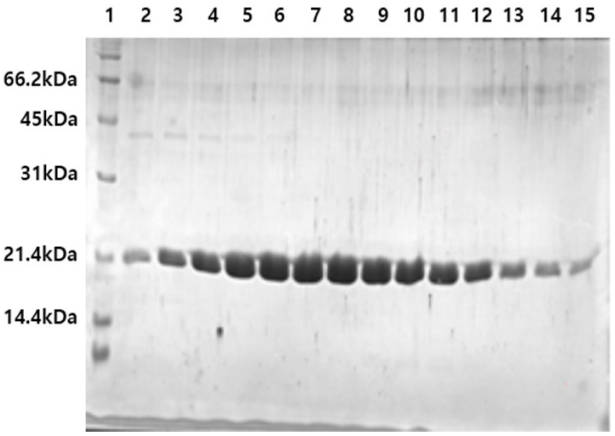

FIGURE 1 | SDS-PAGE of purified DUSP13a. The result of gel filtration chromatography with the DUSP13a. Lane 1, protein size markers; lanes 2-15, fractions of the DUSP13a peak in the gel filtration chromatography. For usage in the crystallization, fractions for lanes 5-12 were pooled and concentrated.

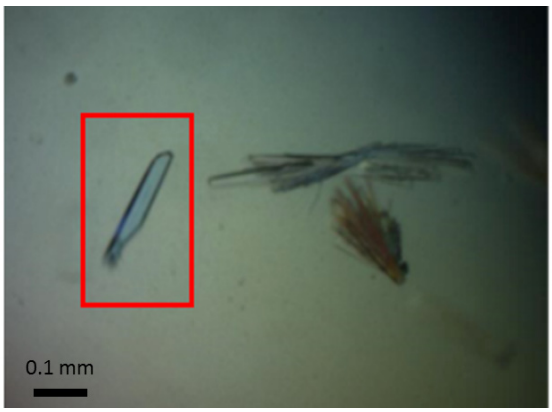

FIGURE 2 | Crystals of DUSP13a. The single crystal of DUSP13a is shown in the red box. The size of the single crystal is about 0.2 mm in the long dimension. The 0.1 mm scale bar is included in the figure.

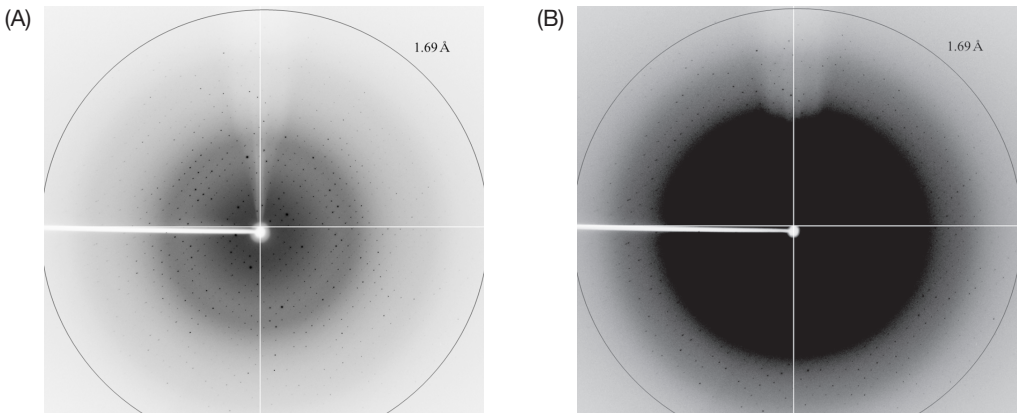

FIGURE 3 | Diffraction pattern. A representative diffraction image of the DUSP13a crystal. Resolution circle for 1.69 Å is included in the image. (A) and (B) are presentations of the same image with different contrasts to show low resolution and high resolution spots, respectively.

system. Cysteines in the DUSP13a gene were mutated to serine or alanine by site mutagenesis (C18A, C35A, C77A, C129S, and C176A) to make a stable protein by preventing cysteine oxidation. Active site cysteine (Cys 129) was mutated to serine while other cysteines to alanines. The phosphatase enzyme activity of the mutant containing the four Cys-to-Ala mutations was comparable to that of the wild type (data not shown), indicating that the mutations did not likely to affect the DUSP13a structure. The Cys-to-Ser mutation of the active site cysteine was shown not to disturb the active site structure of other DUSPs (Jeong et al., 2014). The optimized condition of DUSP13a for induction of overexpression was 0.1 mM IPTG at 37℃ for 3 hours. The His-tagged DUSP13a protein was purified by a Talon crude column. After thrombin cleavage, the protein was further purified by gel filtration chromatography by using a buffer containing 25 mM Tris-HCl (pH 7.5), 200 mM NaCl and 2 mM DTT (Figure 1). Finally, purified DUSP13a was concentrated to 10 mg/ml for crystallization.

Crystal screening was performed by using commercial screening solutions followed with a grid screening with addition of various concentrations of salts and buffers, which yielded crystals of thin plates and clusters. The crystals were improved by adding ethanol in the mother liquor. The number of single crystals increased in the high concentration of ethanol. Usage of other alcohols such as methanol and isopropanol decreased the number of single crystals and the size of crystals. The proper pH range for making good crystals was from 7.5 to 8.5, and pH conditions beyond this range resulted in low quality crystals. The optimal crystallization condition was a mother liquor containing 100 mM Tris-HCl (pH 8.5) and 20% ethanol (Table 1). The best crystals were obtained in the drop of 0.2 μl DUSP13a (10 mg/mL concentration in 25 mM Tris-HCl (pH 7.5), 200 mM

TABLE 1 | Crystallization

Method	Sitting-drop vapor-diffusion
Plate type	96-Well Sitting-Drop Crystallography Plate
Temperature (K)	291
Protein concentration (mg ml)	10
Buffer composition of protein	25 mM Tris-HCl (pH 7.5), 200 mM NaCl and 2 mM DTT
Composition of reservoir solution	100 mM Tris-HCl (pH 8.5) and 20% ethanol
Volume of drop (μl)	0.4 (protein : reservoir = 1:1)
Volume of reservoir (μl)	70

TABLE 2 | Data collection and processing statistics

Diffraction source	Beamline 7A, Pohang Light Source (PLS)
Wavelength (Å)	1.0000
Temperature (K)	100
Space group	$P2_1$
a, b, c (Å)	40.04, 89.34, 45.90
α, β, γ (°)	90.00, 89.87, 90.00
Resolution range (Å)	24.98 - 1.69 (1.72-1.69)*
Completeness (%)	99.9 (93.3)
Redundancy	3.7 (3.7)
R_{merge} (%)	8.7 (30.4)
Average I/σ(I)	31.5 (7.2)

* Statistics in parenthesis are for the highest resolution bin.

NaCl and 2 mM DTT) solution with an equal volume of reservoir solution containing 100 mM Tris-HCl (pH 8.5) and 20% ethanol (Figure 2 and Table 1). The crystal of DUSP13a diffracted to 1.7 Å resolution (Figure 3). Preliminary crystallographic analyses revealed that the space group of the crystal was $P2_1$ with unit cell parameters of a = 40.04 Å, b = 89.34 Å, c = 45.90 Å, α = 90.00°, β = 89.87° and γ = 90.00°. The data collection and processing statistics are shown in Table 2.

METHODS

Cloning and purification of the recombinant proteins

The cDNA coding for human DUSP13a (residues 1–185, Genbank ID: NP_001007272.1) was subcloned into the pET-28a vector by using the forward (5'- GGCC CATATG ATG GCT GAG ACC TCT –3') and reverse (5'- GGCC AAGCTT TCA GGC ACC CCG CAG –3') primers containing restriction enzyme sites (underlined) for NdeI and HindIII, respectively. The PCR product and pET-28a vector were digested with NdeI and HindIII and ligated before transforming *E.coli* BL21(DE3). To minimize cysteine oxidation, cysteines were mutated to alanine or serine (C18A, C35A, C77A, C129S and C176A). The 5-Cys mutations were necessary for stable protein expression and crystallization. Cells were induced with 0.1 mM IPTG at 37°C and grown further for 3 hours. Cells were harvested and then resuspended in a lysis buffer containing 50 mM Tris-HCl (pH 7.5), 500 mM NaCl, 1 mM PMSF and 0.05% (v/v) 2-mercaptoethanol. After cell lysis, the His-tagged DUSP13a protein was purified by the TALON affinity chromatography. His-tag was removed by thrombin digestion, and the protein was then purified by the Sephacryl S-100 gel filtration chromatography with a buffer containing 25 mM Tris-HCl (pH 7.5), 200 mM NaCl and 2 mM DTT. The purified protein was concentrated to 10 mg/mL for crystallization.

Crystallization and X-ray data collection

Crystallization was performed at 18 °C using the sitting-drop vapor-diffusion method. Initial trials were carried out by using commercial screening kits (Hampton Research). The best crystals were grown by mixing 0.2 μl of protein (10 mg/mL) solution and an equal volume of reservoir solution containing 100 mM Tris-HCl (pH 8.5) and 20% ethanol. X-ray diffraction data were collected at the Pohang Accelerator Laboratory Beamline 7A (Park et al., 2017). A single crystal in the droplet was transferred to a cryo-protective buffer (100 mM Tris-HCl (pH 8.5), 20% ethanol and 20% glycerol) and subjected to nitrogen gas stream at 93 K. Diffraction data were integrated and scaled by using the program HKL2000 (Minor et al., 2006). DUSP13a crystals belonged to the space group $P2_1$ with unit cell parameters of a = 40.04 Å, b = 89.34 Å, c = 45.90 Å, α = 90.00°, β = 89.87° and γ = 90.00°.

CONFLICT OF INTEREST

The authors declare that they have no conflict of interest.

ACKNOWLEDGMENTS

We are grateful for the use of beamline 7A at the Pohang Accelerator Laboratory in Korea. This work was supported by the biomedical technology development project, National Research Foundation, KOREA [NRF-2015M3A9B5030302 to SER].

Original Submission: Feb 15, 2018
Revised Version Received: Mar 15, 2018
Accepted: Mar 15, 2018

References

Alonso, A., and Pulido, R. (2016). The extended human PTPome: a growing tyrosine phosphatase family. *FEBS J* **283**, 1404-1429.

Bermudez, O., Pages, G., and Gimond, C. (2010). The dual-specificity MAP kinase phosphatases: critical roles in development and cancer. *Am J Physiol Cell Physiol* **299**, C189-202.

Chen, H.H., Luche, R., Wei, B., and Tonks, N.K. (2004). Characterization of two distinct dual specificity phosphatases encoded in alternative open reading frames of a single gene located on human chromosome 10q22.2. *J Biol Chem* **279**, 41404-41413.

Jeong, D.G., Wei, C.H., Ku, B., Jeon, T.J., Chien, P.N., Kim, J.K., Park, S.Y., Hwang, H.S., Ryu, S.Y., Park, H., Kim, D.S., Kim, S.J., and Ryu, S.E. (2014). The family-wide structure and function of human dual-specificity protein phosphatases. *Acta Crystallogr D Biol Crystallogr* **70**, 421-435.

Katagiri, C., Masuda, K., Nomura, M., Tanoue, K., Fujita, S., Yamashita, Y., Katakura, R., Shiiba, K., Nomura, E., Sato, M., Tanuma, N., and Shima, H. (2011). DUSP13B/TMDP inhibits stress-activated MAPKs and suppresses AP-1-dependent gene expression. *Mol Cell Biochem* **352**, 155-162.

Keyse, S.M. (2008). Dual-specificity MAP kinase phosphatases (MKPs) and cancer. *Cancer Metastasis Rev* **27**, 253-261.

Kim, S.J., Jeong, D.G., Yoon, T.S., Son, J.H., Cho, S.K., Ryu, S.E., and Kim, J.H. (2007). Crystal structure of human TMDP, a testis-specific dual specificity protein phosphatase: implications for substrate specificity. *Proteins* **66**, 239-245.

Minor, W., Cymborowski, M., Otwinowski, Z., and Chruszcz, M. (2006). HKL-3000: the integration of data reduction and structure solution - from diffraction images to an initial model in minutes. *Acta Crystallogr D Biol Crystallogr* **62**, 859-866.

Nakamura, K., Shima, H., Watanabe, M., Haneji, T., and Kikuchi, K. (1999). Molecular cloning and characterization of a novel dual-specificity protein phosphatase possibly involved in spermatogenesis. *Biochem J* **344 Pt 3**, 819-825.

Park, J.E., Park, B.C., Kim, H.A., Song, M., Park, S.G., Lee, D.H., Kim, H.J., Choi, H.K., Kim, J.T., and Cho, S. (2010). Positive regulation of apoptosis signal-regulating kinase 1 by dual-specificity phosphatase 13A. *Cell Mol Life Sci* **67**, 2619-2629.

Park, S.-Y., Ha, S.-C., and Kim, Y.-G. (2017). The protein crystallography beamlines at the Pohang Light Source II. *Biodesign* **5**, 30-34.

Patterson, K.I., Brummer, T., O'Brien, P.M., and Daly, R.J. (2009). Dual-specificity phosphatases: critical regulators with diverse cellular targets. *Biochem J* **418**, 475-489.

Pavic, K., Duan, G., and Kohn, M. (2015). VHR/DUSP3 phosphatase: structure, function and regulation. *FEBS J* **282**, 1871-1890.

Tonks, N.K. (2006). Protein tyrosine phosphatases: from genes, to function, to disease. *Nat Rev Mol Cell Biol* **7**, 833-846.

Wiesmann, C., Barr, K.J., Kung, J., Zhu, J., Erlanson, D.A., Shen, W., Fahr, B.J., Zhong, M., Taylor, L., Randal, M., McDowell, R.S., and Hansen, S.K. (2004). Allosteric inhibition of protein tyrosine phosphatase 1B. *Nat Struct Mol Biol* **11**, 730-737.

Yuvaniyama, J., Denu, J.M., Dixon, J.E., and Saper, M.A. (1996). Crystal structure of the dual specificity protein phosphatase VHR. *Science* **272**, 1328-1331.